6-1-1992

Synchronization in M-PSK Modems

William Osborne
osborne@engr.siu.edu

Brian Kopp
New Mexico State University - Main Campus

Published in Osborne, W., & Kopp, B. (1992). Synchronization in M-PSK modems. IEEE International Conference on Communications, 1992. ICC 92, Conference record, SUPERCOMM/ICC '92, Discovering a New World of Communications, v.3 1436-1440. doi: 10.1109/ICC.1992.268109

SYNCHRONIZATION IN M-PSK MODEMS

By
William Osborne
Brian Kopp
New Mexico State University
Las Cruces, New Mexico

Abstract

In many applications, it is economical for a single modem to receive multiple modulation formats. In particular, the use of BPSK and QPSK has become a defacto standard in many military and NASA systems. However, there is significant interest in employing 8PSK and 16PSK modulation in these same systems today in order to conserve bandwidth.

This paper addresses a technique for achieving carrier synchronization for all four of these PSK schemes in a single modem. This is accomplished by using quadrature channel carrier recovery processing and a version of the MAP phase detector algorithm. A model for the simulation of this tracking process is derived and results are presented to confirm its functionality.

Introduction

In a multi-modulation environment it is advantageous to consider the use of a single carrier tracking system. The complexity of synchronous communication systems alone warrant this consideration. Further, concern for limited space, cost, and power strengthen the argument in favor of a single tracking system. The first part of this paper, Carrier Tracking, discusses the use of maximum aposteriori estimation (MAP) in quadrature carrier recovery decision directed loops. Further, the use of digital circuitry in achieving multi-mode PSK synchronization is addressed. In the second part, A Baseband Model For Carrier Tracking, a model is developed for considering the tracking process in terms of carrier phase error. The tracking loop model is second order and additive white Gaussian noise is assumed for each of the two quadrature channels. This model lends itself quite well to simulation. A program was created to simulate the tracking loop and the variance in the phase error for a practical range of signal-to noise ratios (SNR) is presented for all four modulation schemes in the third part of this paper; Simulating the Baseband Model. The simulated variance data is compared with theoretical data for each of the modes. The approach that was used for obtaining the theoretical data is presented in Appendix A.

Carrier Tracking

The Costas crossover loop is typically used in the tracking of BPSK and QPSK signals. However, the hard-limiters employed by the loop make it inappropriate for use in higher order modulation schemes such as 8 and 16-PSK systems where the modulation data takes on values other than ± 1. The use of decision directed loops that employ maximum aposteriori estimation techniques has been proposed for tracking of MPSK modulation [1]. The technique employs a quadrature channel carrier recovery loop and a polar phase estimator. Using the output of the quadrature channel matched filters, the polar phase estimator makes a hard decision as to what modulation data was transmitted during the last symbol period. This estimate is then used in conjunction with the filter outputs to generate an error signal. The error signal is passed to a loop filter and VCO which generates the local carrier reference for demodulation. Figure 1 shows the block diagram of the MAP estimation loop.

The MAP estimator performs several functions in making its decision as to what was transmitted. First it obtains the phase angle that is conveyed with I and Q by taking the arctangent of the ratio Q/I. The angle is then compared with each possible modulation angle (e.g., in 8PSK the modulation angles could be chosen as $\pi/16$, $3\pi/16$, $5\pi/16$, $7\pi/16$, $9\pi/16$, $11\pi/16$, $13\pi/16$, and $15\pi/16$). The modulation angle that is closest to the received angle is selected as the maximum aposteriori estimate to the transmitted angle. The cosine and sine of the estimate, $\hat{I}$ and $\hat{Q}$, are taken and used to generate an error signal.

To form the error signal the output of the I and Q matched filters are multiplied by the sine and cosine angle estimates, respectively. This is shown in Figure 1. The difference between the two products is the error signal. This is shown, in Figure 1, as the input to the filter. In the absence of symbol errors this is the traditional PLL tracking error quantity which occurs with a mixing phase detector and pure sine-wave inputs. With the use of a filter whose Laplace transform is 1+a/s and in the absence of symbol errors this tracking system performs identically to a 2nd order PLL.

The use of the MAP estimator in an MPSK modem can be easily implemented using digital logic. The I and Q channels are sampled and the digital information is passed to a set of erasable-programmable-read-only-memories (EPROM). The EPROM is used not only to generate the MAP estimates of I and Q but to perform the error signal calculation as well. Further, digital integrate and dump filters, EPROMs, a digital loop filter, and a numerically controlled oscillator (NCO) can be used to simplify the implementation. The use of digital circuitry can greatly reduce the complexity of the overall modem design. Selecting the modulation type is simply a matter of selecting the correct EPROM addresses for the phase detector output.

Baseband Model For Carrier Tracking

Consider the input to the synchronizer in Figure 1 as

$$r(t) = s(t) + w(t) \tag{1}$$

where s(t) is the M-PSK transmitted signal

$$s(t) = \sqrt{\frac{2E_s}{T}} \cos(\omega_c t + \theta_m + \varphi_i) \tag{2}$$

This work was supported by NASA grant # NAG5-1491

and w(t) is white noise with power spectral density $\frac{N_0}{2}$. The energy per symbol is denoted as E_s and the symbol period is T. The carrier frequency is ω_c and the M-PSK symbol that is transmitted is designated as θ_m where

$$\theta_m = \frac{2\pi i}{M} \qquad i = 0,1,.....M-1 \qquad (3).$$

The term φ_i is the phase offset of the received signal. The corresponding integrator outputs are

$$I = g\int_0^T r(t)\cos(\omega_c t + \varphi_o) \quad \text{and}$$

$$Q = g\int_0^T r(t)\sin(\omega_c t + \varphi_o) \qquad (4)$$

where φ_o is the phase offset of the reference VCO and g is the gain of the integrators. These two equations can be rewritten as

$$I = I_s + N_i \quad \text{and} \quad Q = Q_s + N_q \qquad (5)$$

where N_i and N_q are zero mean Gaussian random variables with equal variances of $\sigma^2 = \frac{N_0}{2E_s}$. To evaluate I_s and Q_s we let $g = \sqrt{\frac{2}{E_s T}}$ and $\varphi = \varphi_i - \varphi_o$. Now performing the integration and inserting the values for g and φ we have

$$I_s = \cos(\theta_m + \varphi) \quad \text{and} \quad Q_s = \sin(\theta_m + \varphi) \qquad (6).$$

Since the signal components I_s and Q_s are separate from their corresponding noise terms N_i and N_q, the error signal

$$e(t) = Q\hat{I} - I\hat{Q} \qquad (7)$$

becomes

$$e(t) = Q_s\hat{I} + N_q\hat{I} - I_s\hat{Q} - N_i\hat{Q} \qquad (8).$$

The tracking loop's error signal is comprised of two quantities of information. The phase detector characteristic and a noise term. The phase detector characteristic is the expected value of the error signal and since the noise terms N_i and N_q have expected values of 0

$$PD(\varphi) = E[e(t)] = E\left[Q_s\hat{I} - I_s\hat{Q}\right] \qquad (9).$$

The error signal can now be expressed as

$$e(t) = PD(\varphi) + N_e(t) \qquad (10)$$

where $N_e(t) = N_q\hat{I} - N_i\hat{Q}$ (11).

Having obtained an expression for the error function in terms of the phase detector characteristic the baseband model can now be constructed as shown in Figure 2(a). The phase offset from the VCO is subtracted from the received phase and this difference is what is passed to the phase detector. The noise term $N_e(t)$ is subsequently added and the result is passed to the loop filter.

Simulating the Baseband Model

Figure 2(b) shows the modification to the baseband model that is made to perform a simulation of the tracking loop. In effect, equation (8) is calculated to determine the error signal. The noise terms and the data are obtained using simple random number generators. The error is passed to a discrete time transfer function that performs the filtering and VCO integration. The resulting phase is retained for the following iteration. It should be noted that the phase detector gain at high SNR was fixed at 1.

The simulator that was constructed utilizes the C programming language. To consider the use of digital circuitry in an implementation of this synchronization system I and Q are quantized before $\hat{I}$ and $\hat{Q}$ are calculated. This quantization is done

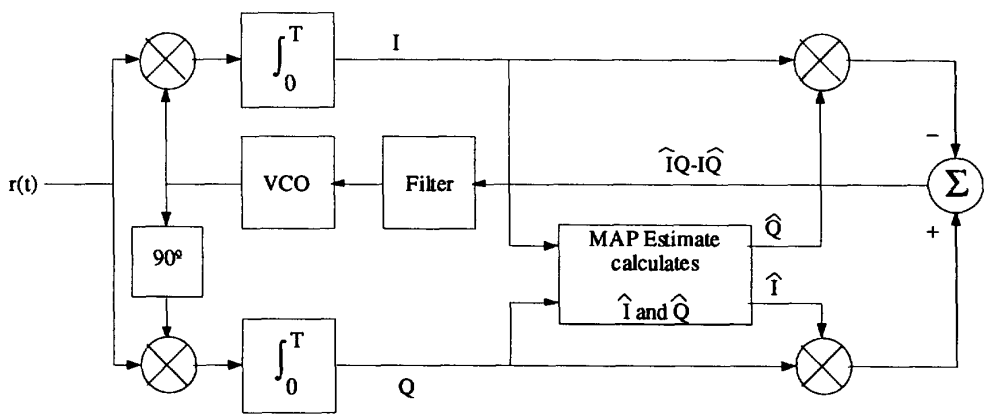

Figure 1. MAP estimation loop block diagram.

in a manner consistent with a demodulator and synchronizer currently being implemented by the authors. To demonstrate that the simulations were accurate, normalized step responses of the carrier tracking loop simulator for BPSK, QPSK, 8PSK, and 16 PSK formats and random data were obtained. These simulator responses were compared to theoretical responses [2, p. 49] and determined to be accurate.

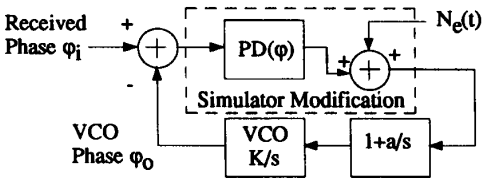

Figure 2(a). The baseband model.

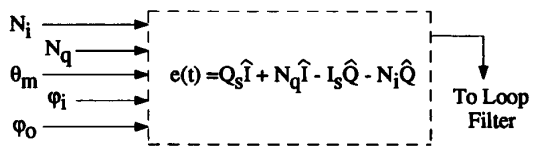

Figure 2(b). The Simulator modification.

The most important performance parameter associated with carrier tracking loops is the phase jitter in the loop versus SNR, since the jitter results in detection performance loss. The variance is due to two factors. The first occurs in all PLLs and reflects the presence of noise in the incoming signal. The second factor is attributable to the use of a particular type of carrier tracking loop, in this case a decision directed loop. This second factor is most often referred to as the squaring loss. Its theoretical calculation for the modem's MPSK MAP estimation carrier tracking loops is presented in Appendix A.

The simulator was used to measure the variance in the phase error versus SNR and these results are shown in Figures 3 and 4. The first plot shows the variance in phase error for BPSK and QPSK. The theoretical approximations for the variances, using the approach in Appendix A are plotted as well. Figure 4 shows the variance in phase error for 8 PSK and 16 PSK. The quantity, E_s/N_o , present in the plots, is PSK symbol energy to noise spectral density. Figure A-4 shows the theoretical squaring loss calculations for all four modulation techniques. Note, the very large differences in squaring loss between the various schemes. At a SNR where squaring loss may be negligible for BPSK it can be prohibitory for 16 PSK. Operating at an E_s/N_o of 10 dB incurs no loss in loop performance due to squaring loss for BPSK but for 16 PSK there is a more than 40 dB loss in loop performance that must be considered.

One aspect of the simulation that is worth noting is the change in loop noise bandwidth that occurs in the simulator as the SNR changes with constant signal level (perfect AGC). Since the phase detector gain is a function of error rate and hence SNR, as the SNR drops the phase detector gain drops and the corresponding loop noise bandwidth gets smaller. This in effect lowers the amount of jitter that is present when compared to a similar calculation made with a fixed loop bandwidth. The theoretical calculations of phase jitter based upon squaring loss and a linear model must take into account the changing loop noise bandwidth that occurs in the simulator (and in most actual loops), if they are to be compared with the phase error variances of the simulator. This was done for our theoretical results in Figures 3 & 4. It is interesting to note that this aspect of the simulator more actually mimics practice than the theory does. As a rule, the phase detector gain of a carrier tracking loop is not modified on the fly to account for a changing SNR operating condition in an attempt to keep the loop noise bandwidth constant.

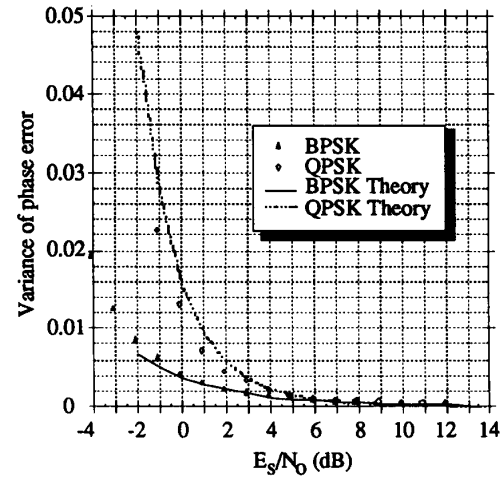

Figure 3. Phase error variance for BPSK and QPSK in high SNR loop with loop BW = 6250 Hz for 1 MHz symbol rate

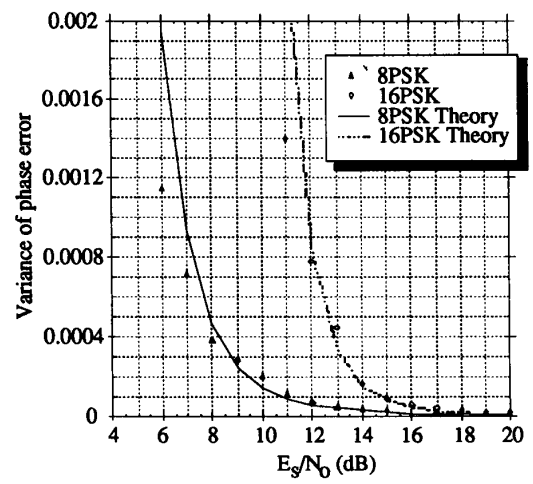

Figure 4. Phase error variance for 8PSK and 16PSK in high SNR loop with loop BW = 1250 Hz for 1 MHz symbol rate

Appendix A: Carrier Tracking Loop Squaring Loss

One of the more popular techniques for analyzing the jitter performance of carrier tracking loops is to linearize the loop and evaluate the resulting variance of the phase error. For the MAP loops of interest in this paper the resulting phase error variance can be expressed as

$$\sigma_\varphi^2 = \frac{No}{2Es}\frac{BL}{SR} \cdot SL^{-1} \qquad \text{(A-1)}$$

where Es/No is the ratio of the energy per symbol to noise spectral density, SR is the symbol rate, BL is the loop noise bandwidth, and SL is the "squaring loss" of the phase detector. The "squaring loss" (the term was originally applied to BPSK) is the increase in phase jitter within the loop over a conventional PLL of the same bandwidth due to the nonlinearity involved in the phase detection process, i.e. the phase detector output PD is given by

$$PD(\varphi) = Q\hat{I} - I\hat{Q} \qquad \text{(A-2)}$$

where, I & Q are the analog outputs of the I & Q channel matched jitters, $\hat{I}$ & $\hat{Q}$ are the hard decision channel outputs and φ is the phase error. The squaring loss for BPSK and QPSK can be found in the literature [11, 12]. For 8 and 16 PSK no analytical result is readily available. The squaring loss is generated from two physical actions and these are:

(1) The phase detector gain (even at constant signal levels) depends upon the SNR through $\hat{I}$ and $\hat{Q}$ and goes down as the error rate goes up. This increases the jitter in the loop because there is less signal to track at a given SNR.

(2) The variance of the equivalent noise term in the loop is affected by the presence of errors also. Generally, this effect lessens the phase error by a slight amount.

The affects upon the variance of noise are very secondary, as we will soon show for a QPSK loop. It can be shown by linear loop analysis that the squaring loss neglecting the effects of errors on the noise term is given by

$$SL\ (SNR) = 1/G^2 \qquad \text{(A-3)}$$

where G is the gain of the phase detector at zero phase error normalized to one at high SNR. The model used for evaluating phase detector gain is shown in figure A-1. With this model I & Q are ready shown to be independent gaussian random variables with statistics given by

$$m_I = Cos(\theta_m + \varphi) \qquad \sigma_I^2 = \frac{No}{2E_s}$$

$$m_Q = -Sin(\theta_m + \varphi) \qquad \sigma_Q^2 = \frac{No}{2E_s}$$

The phase detector characteristic, $PD(\varphi)$, is the expected value of the error signal shown in figure A-1, i.e.,

$$PD(\varphi) = E(I Sin\theta_m - Q\ Cos\theta_m) \qquad \text{(A-4)}$$

To see how the phase detector works consider the no noise case and a static phase error of φ which is small compared to $2\pi/M$. Then

$$I = Cos(\theta_m + \varphi)$$

$$Q = -Sin(\theta_m + \varphi)$$

$$\hat{\theta} = \theta_m$$

and PD (φ) is given by

$$PD(\varphi) = Cos(\theta_m + \varphi)Sin\theta_m + Sin(\theta_m + \varphi)Cos\theta_m$$

or $PD(\varphi) = Sin(\varphi)$ for no noise. (A-5)

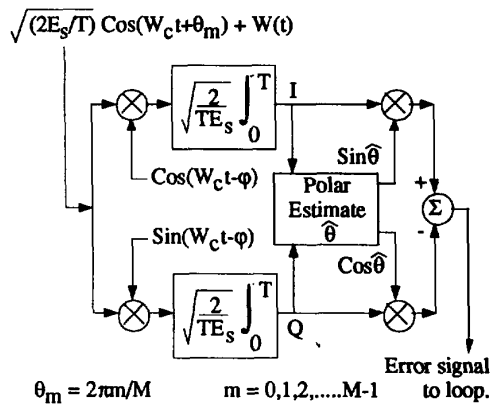

Figure A-1. Phase detector gain evaluation model.

Of course, if the phase error is larger than π/M then $\hat{\theta}$ will be equal to the value of modulation phase nearest to $\theta_m + \varphi$ and thus the phase detector characteristic is periodic in φ with period of $2\pi/M$. The phase detector characteristic in A-3 can be evaluated by averaging over the noise and the data as follows

$$PD(\varphi) = E\ \{[Cos(\theta_m + \varphi) + N_I]Sin\hat{\theta} + [Sin\ (\theta_m + \varphi) + N_Q]\ Cos\hat{\theta}\}$$

or $PD(\varphi) = E\{Sin(\varphi - \frac{2\pi i}{M})\}$ (A-6)

where i is the hard decision at the output of the polar estimator. It follows that

$$PD(\varphi) = \sum_{i=0}^{M-1} Pr(i|0) \sin\left(\varphi - \frac{2\pi i}{M}\right) \qquad \text{(A-7)}$$

where we have fixed the transmitted data symbol at zero since $PD(\varphi)$ is totally symmetrical with respect to transmitted symbols and $Pr(i|0)$ is the probability of a hard decision on phase being in the ith sector given $\theta_m = O$. This expression can be evaluated for all forms of MPSK using the fact that the density function of phase is given by [13]

$$r(\psi) = \frac{1}{2\pi} e^{-Es/No} \left[1 + Z\sqrt{2\pi}\, e^{Z^2/2}\, Q(-Z)\right]$$

$$Z = \sqrt{\frac{2Es}{No}} \cos(\psi) \qquad \text{(A-8)}$$

and performing the indicated integration of A-8 numerically to obtain $Pr(i|0)$. A typical set of phase detector characteristics are shown in Figure A-2 for an 8PSK loop. The periodicity and the gain reduction with decreasing SNR are apparent. The gain of the phase detector is obtained by calculating the slope of $PD(\varphi)$ at φ=0. The resulting squaring loss for QPSK is shown in figure A-3 for this technique and a more exact analysis from [12]. As discussed previously the squaring loss given by our approximation and the result including the effects of noise correlation are within .5dB in Es/No of each other for all reasonable values of Es/No. The squaring loss calculated by this technique for all 4 loop types is shown in figure A-4 this result is used in the section on carrier tracking to provide a theorical estimate of the loop phase jitter.

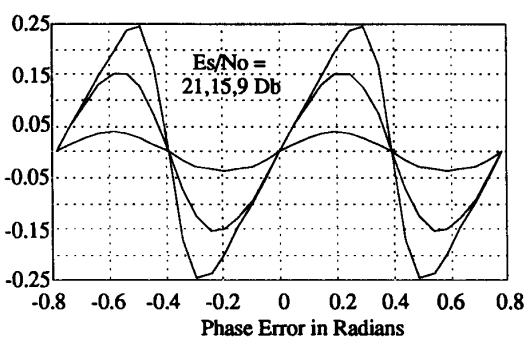

Figure A-2. Phase detector for 8PSK MAP loop.

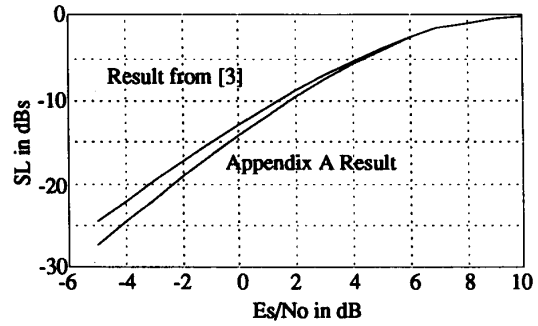

Figure A-3. Squaring loss for high SNR QPSK MAP loop.

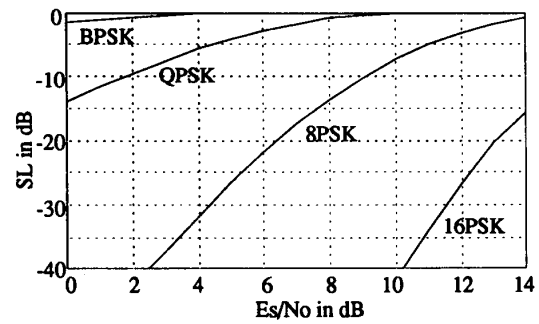

Figure A-4. MPSK squaring loss for MAP loop.

References

1. M. K. Simon, "Further Results on Optimum Receiver Structures for Digital Phase and Amplitude Modulated Signals," in Proceedings of the International Communications Conference, 1978, pp. 42.1.1 -42.1.7.

2. F. M. Gardner, Phaselock Techniques, New York: John Wiley & Sons, 1979.

3. J.H. Yuen, "Deep Space Telecommunications Systems Engineering', Plenum Press, 1983.

4. Hinedi, S., Lindsey, W.C., "On the Noise In QPSK Decision-Feedback Carrier Tracking Loops", IEEE Transactions on Communications, Vol. 37, April 1989.

5. Parsons, R.D. and Wilson, S.G., "Polar Quantizing for Coded PSK Transmission", IEEE Transcation on Communications, Vol. 38, Sept. 1990.